INORGANIC CHEMISTRY
FRONTIERS

RESEARCH ARTICLE

View Article Online
View Journal | View Issue

Cite this: *Inorg. Chem. Front.*, 2022, **9**, 4614

$Li_{6.58}Na_{7.43}Sr_4(B_9O_{18})(B_{12}O_{24})Cl$: unprecedented combination of the largest two highly polymerized isolated B–O clusters with novel isolated B_9O_{18} FBB†

Feixiang Wang, [a,b] Yun Yang, *[a,b] Congcong Jin[a,b] and Shilie Pan *[a,b]

Received 20th June 2022,
Accepted 26th July 2022

DOI: 10.1039/d2qi01311h

rsc.li/frontiers-inorganic

A new borate, $Li_{6.58}Na_{7.43}Sr_4(B_9O_{18})(B_{12}O_{24})Cl$ (LNSBOC), was successfully obtained *via* a spontaneous crystallization method in an open system. LNSBOC crystallizes in a hexagonal crystal system with the centrosymmetric space group of $P6_3/m$, with a = 9.3046(2) Å, c = 24.3239(7) Å and Z = 2. According to the statistics, the structure of LNSBOC is extraordinary not only because of the discovery of the novel fan-like fundamental building block B_9O_{18}, but also for the unprecedented coexistence of the largest two highly polymerized (number of B atoms more than six) isolated B–O clusters in the structure. A discussion about the cause of the rareness of borates containing two polymerized isolated B–O clusters was carried out by investigating previous research and extant compounds. Even more significantly, a strategy to design compounds/crystal structures containing two polymerized isolated B–O clusters is put forward in this work from the viewpoint of structures and elements. In addition, thermal analysis and infrared and UV–Vis–NIR diffuse reflectance spectroscopy were performed for the title compound.

Introduction

Over the past few decades, borates have become a research hot spot worldwide owing to their extended structural diversity and application potential in the fields of nonlinear optical materials, luminophores, ferroelectric and piezoelectric materials, and semiconductors.[1–13] There exist three coordination environments of boron, including two, three and four coordinated with oxygen atoms to form linear BO_2, triangular BO_3 and tetrahedral BO_4 basic units.[14–21] The above basic units can further connect by corner-sharing or/and edge-sharing methods, which results in a large number of anionic polymeric borate groups, including isolated clusters, chains, rings, sheets, and framework structures.[22–27] The variety of borates' structures leads to their unique properties and makes it easy for scientists to design and synthesize new compounds.[28–37]

Among all sorts of the above structures, borates with isolated B–O clusters (I-borates)[38] attract researchers' attention because they are likely to possess outstanding properties. It is also mentioned in previous research that borates with isolated BO_3 and B_3O_6 clusters arranged along the same direction always have relatively large birefringence and the second-harmonic generation (SHG) effect.[39–42] As proof, $KBe_2BO_3F_2$ (KBBF)[43] with isolated BO_3 units was the only nonlinear optical crystal that can practically output deep-ultraviolet (deep-UV) coherent light by the direct SHG process, until now.[44] And α-BaB_2O_4[45–47] with isolated B_3O_6 clusters has already realized commercial application as an excellent birefringent crystal. Apart from their properties, I-borates could also furnish a possible way to investigate the mechanism of the regulating effect and controlling effect derived from cations in the meantime.[48,49]

According to the statistical analysis conducted by Mutailipu *et al.*,[50] I-borates comprise 65.5% of the 965 screened anhydrous borates, which illustrates that I-borates are a vital part of borates. The frequency distribution conformed well to the former work summarized by Becker[25] in 2001 and Yuan[51] *et al.* in 2007 and the same point of view could also be drawn. Normally, I-borates contain only one sort of isolated B–O cluster, for instance, $Sr_2Be_2B_2O_7$ (SBBO)[52] and $Li_4Sr(BO_3)_2$[53] with isolated BO_3 units, β-BaB_2O_4[54] with isolated B_3O_6 clusters,

[a]*Research Center for Crystal Materials, CAS Key Laboratory of Functional Materials and Devices for Special Environments, Xinjiang Technical Institute of Physics & Chemistry, CAS, 40-1 South Beijing Road, Urumqi 830011, China. E-mail: slpan@ms.xjb.ac.cn*

[b]*Center of Materials Science and Optoelectronics Engineering, University of Chinese Academy of Sciences, Beijing 100049, China*

† Electronic supplementary information (ESI) available: CIF files, table of atomic coordinates, equivalent isotropic displacement parameters, bond valence sum, selected bond distances and angles, and structure comparison. CCDC 2177205 for $Li_{6.58}Na_{7.43}Sr_4(B_9O_{18})(B_{12}O_{24})Cl$. For the ESI and crystallographic data in CIF or another electronic format see DOI: https://doi.org/10.1039/d2qi01311h

$KZnB_3O_6$[55] with isolated B_6O_{12} clusters, $Li_6Rb_5B_{11}O_{22}$[56] with isolated $B_{11}O_{22}$ clusters, *etc*. Furthermore, this could also be proved by the fact that only 35 compounds (including the title compound) in anhydrous borates possessed two types (or more) of isolated clusters at the same time until now. There exists only one case of a compound, $Ba_6Al_4B_{14}O_{33}$,[57] which contains three different kinds of isolated clusters, BO_3, B_6O_{13} and B_6O_{14}. These cases are rare and disobey Pauling's 5th rule that the number of essentially different kinds of structural units in a crystal tends to be the least.[58,59] In order to diminish the conflict with Pauling's 5th rule, the coexisting B–O clusters are inclined to form similar structures.[38] Meanwhile, I-borates with large isolated B–O clusters are seldom observed experimentally, which is in vivid contrast to the large quantity of I-borates. It could be proved by statistics that 419 borates with only isolated BO_3 units comprise 66.3% of the above I-borates and about 97.0% of anhydrous borates contain isolated B–O clusters with a number of B atoms less than six in their fundamental building blocks (FBBs).[50] Furthermore, the rareness of the existence of highly polymerized (number of B atoms more than six) B–O clusters can be observed in the above 35 I-borates with two kinds (or more) of B–O clusters as well. Except for the title compound, none of them contain two highly polymerized B–O clusters at the same time. Eventually, a conclusion could be drawn from the above statistical data and experimental examples that borates containing more than one sort of highly polymerized isolated cluster are quite extraordinary and unprecedented.

Herein, $Li_{6.58}Na_{7.43}Sr_4(B_9O_{18})(B_{12}O_{24})Cl$ (LNSBOC), a new borate containing two highly polymerized isolated B–O clusters (B_9O_{18} and $B_{12}O_{24}$), was successfully synthesized *via* a spontaneous crystallization method in an open system. Based on our inquiry, LNSBOC has exhibited the largest two highly polymerized isolated B–O clusters in I-borates with two kinds of B–O clusters so far. At the same time, the isolated B_9O_{18} cluster is a novel FBB observed for the first time. In this work, several factors which possibly lead to the rareness of borates containing two polymerized isolated B–O clusters are displayed, and we also put forward a strategy to design this kind of compound. Moreover, the synthesis, crystal structure, thermal behaviors, and spectral properties of the title compound are reported too.

Experimental section

Synthesis

$LiBO_2$ (Aladdin, 99.9%), NaCl (Tianjinshi Baishi Chemical Co. Ltd, ≥99.5%), Na_2CO_3 (Aladdin, 99.5%), $SrCO_3$ (Aladdin, 99%) and B_2O_3 (Aladdin, 98%), H_3BO_3 (Aladdin, ≥99.5%) were gathered from commercial sources, and no further purification was implemented.

Single crystals of LNSBOC were grown by the spontaneous crystallization method in an open system. The raw materials, $LiBO_2$, NaCl, Na_2CO_3, $SrCO_3$ and B_2O_3, were well ground in a ratio of 12 : 2 : 7 : 8 : 15 and then put into a platinum crucible. It was gradually heated to 700 °C for 7 hours and kept at this temperature for 24 hours to ensure complete melting. The solution was slowly cooled to 550 °C at a rate of 1.5 °C h^{-1}, and then the slow cooling proceeded with a rate of 2 °C h^{-1} to 400 °C. After that, it was rapidly cooled to room temperature at a rate of 7.5 °C h^{-1} and then colourless crystals of LNSBOC were obtained.

A polycrystalline powder of LNSBOC was prepared *via* the conventional solid-state reaction method in an open system. The raw materials $LiBO_2$, NaCl, Na_2CO_3, $SrCO_3$ and H_3BO_3 were ground with a stoichiometric ratio in a clean mortar, then placed in an aluminium trioxide crucible and preheated at 300 °C for 10 hours, and then heated to 560 °C and held at this temperature for 72 hours. After these sintering steps, the sample was brought down to room temperature at a rate of 20 °C h^{-1}. Then the purity of the sample was determined using a Bruker D2 PHASER diffractometer with Cu Kα radiation at room temperature. Diffraction patterns were recorded in the range 2θ = 10–70° with a scan step width of 0.02° and a scan rate of 1 s per step. Compared with the theoretical simulation of the powder pattern generated by calculating the interplanar spacing and crystal plane position from the crystal structure data, it could be concluded that the polycrystalline powder of LNSBOC is pure (Fig. 1).

Single crystal X-ray diffraction

Colourless, block-shaped single crystals with the appropriate size of LNSBOC were selected under an optical microscope for structural characterization. Single-crystal XRD data were collected using a Bruker D8 Venture diffractometer with Mo Kα radiation (λ = 0.71073 Å), and the data were integrated using the SAINT program.[60] The structure was solved with Olex2 and SHELXTL by direct methods.[61,62] The full matrix least squares method was also used to refine the positions of all atoms. The Na(2) atomic sites were in disorder; therefore, the Na(2A) and Li(2A) atoms were set to share the same sites. PLATON was used to examine the possible higher symmetry of the structure, but no higher symmetry was found.[63] Detailed information on

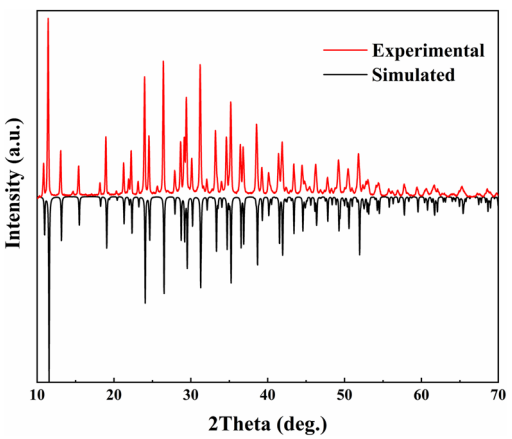

Fig. 1 The calculated and experimental powder-XRD patterns of LNSBOC.

Table 1 Crystal data and structure refinement for LNSBOC

Parameters	Values
Empirical formula	$Li_{6.58}Na_{7.43}Sr_4(B_9O_{18})(B_{12}O_{24})Cl$
Formula weight	1501.27
Temperature	300 K
Wavelength	0.71073 Å
Crystal system, space group	Hexagonal, $P6_3/m$
Unit cell dimensions	a = 9.3046(2) Å c = 24.3239(7) Å
Volume	1823.72(9) Å^3
Z	2
Calculated density	2.734 g cm^{-3}
Absorption coefficient	6.126 mm^{-1}
F(000)	1423
Crystal size	0.22 × 0.12 × 0.05 mm^3
Theta range for data collection	2.528 to 27.478°
Limiting indices	$-11 \le h \le 12$, $-12 \le k \le 12$, $-31 \le l \le 31$
Reflections collected/unique	12 437/1429 [$R_{(int)}$ = 0.0447]
Completeness to theta	99.9%
Refinement method	Full-matrix least-squares on F^2
Goodness-of-fit on F^2	1.141
Data/restraints/parameters	1429/0/130
Final R indices [$F_o^2 > 2\sigma(F_o^2)$]^a	R_1 = 0.0345, wR_2 = 0.0848
R indices (all data)^a	R_1 = 0.0385, wR_2 = 0.0869
Largest diff. peak and hole	0.591 and −1.334 e Å^{-3}

$^a R_1 = \sum||F_o| - |F_c||/\sum|F_o|$ and $wR_2 = [\sum w(F_o^2 - F_c^2)^2/\sum wF_o^4]^{1/2}$ for $F_o^2 > 2\sigma(F_o^2)$.

the structural data is given in Table 1, and the redefined atomic positions, equivalent isotropic displacement parameters and bond valence are listed in Table S1 in the ESI.† The information on the selected bond lengths and angles is given in Table S2 in the ESI.†

Infrared (IR) spectroscopy

Infrared (IR) spectra were recorded on a Shimadzu IR Affinity-11 Fourier transform IR spectrometer in the range from 400 to 4000 cm^{-1} with a resolution of 1 cm^{-1}. The sample was mixed thoroughly with 500 mg of dried KBr.

Energy dispersive X-ray spectroscopy

Elemental analysis of LNSBOC was carried out on the surface of a clean single crystal with the aid of a field emission scanning electron microscope (SEM, SUPRA 55 VP) equipped with an energy dispersive X-ray spectroscope (EDS, BRUKER X-flash-sdd-5010).

UV–Vis–NIR diffuse reflectance measurements

The UV–Vis–NIR diffuse-reflectance spectroscopy data in a wavelength range of 200–2600 nm were recorded at room temperature using a powder sample of LNSBOC on a Shimadzu SolidSpec-3700DUV spectrophotometer. Tetrafluoroethylene was used as a diffuse reflectance standard.

Thermal analysis

Thermal gravimetry (TG) and differential scanning calorimetry (DSC) were carried out to examine the thermal stability of LNSBOC on a simultaneous NETZSCH STA 449 F3 thermal analyzer instrument under a flowing N_2 atmosphere. The sample was placed in a Pt crucible and heated from 40 to 800 °C at a rate of 5 °C min^{-1}.

Results and discussion

Crystal structure

LNSBOC crystallizes in a hexagonal crystal system with the centrosymmetric space group of $P6_3/m$ (No. 176), with a = 9.3046(2) Å, c = 24.3239(7) Å and Z = 2. In the asymmetric unit of LNSBOC, there exist one lithium atom, one sodium atom, two strontium atoms, four boron atoms, eight oxygen atoms, one chlorine atom and one common site of the sodium/lithium atom. In the structure of LNSBOC, there exist two different kinds of B coordination environments, triangular BO_3 and tetrahedral BO_4. It exhibits a complicated three-dimensional network composed of Na(2A)/Li(2A)O_6, Na(1)O_5Cl, Sr(1)O_9, Sr(2)O_6, Li(1)O_4 polyhedra, B_9O_{18} and $B_{12}O_{24}$ groups which are interconnected *via* corner or edge sharing as shown in Fig. 2, 3 and Fig. S1 in the ESI.† Meanwhile, all B_9O_{18} and $B_{12}O_{24}$ groups are isolated from one another and act as two different kinds of FBBs. The B–O bond lengths and angles of triangular BO_3 are in the ranges 1.330(4)–1.401(4) Å and 118.5(3)–122.6(3)°, and the ranges are 1.446(6)–1.485(4) Å and 104.7(3)–113.3(4)° for tetrahedral BO_4, respectively. The Li(1)–O bond distances range from 1.857(7) to 2.186(7) Å. The Na(1)–O bond distances range from 2.285(3) to 2.648(3) Å, the Na(2A)/Li(2A)–O bond distances range from 2.243(3) to 2.357(3) Å, and the Na(1)–Cl bond distance is 2.9699(15) Å. The Sr–O bond distances range from 2.439(2) to 2.914(2) Å.

The isolated fan-like FBB B_9O_{18} is composed of three B_3O_7 units connected by shared O atoms. To the best of our knowledge, isolated B_9O_{18} (9 : 6Δ + 3T)[64] has been obtained for the first time. Although a fan-like B_9O_{18} group was mentioned in Dong's work,[65] it was not isolated and was described as a connecting unit between the double layers rather than a sort of FBB (Fig. S2 in the ESI†). And the isolated petal-like FBB $B_{12}O_{24}$ (12 : 6Δ + 6T)[64] is a circle polyborate containing six triangular BO_3 and six tetrahedral BO_4, which are alternately

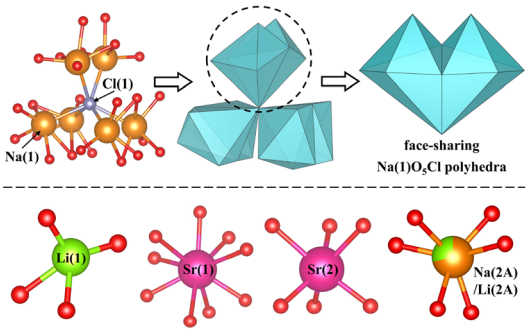

Fig. 2 Face-sharing Na(1)O_5Cl polyhedra and the coordination environments of the Li, Na and Sr atoms in the title compound.

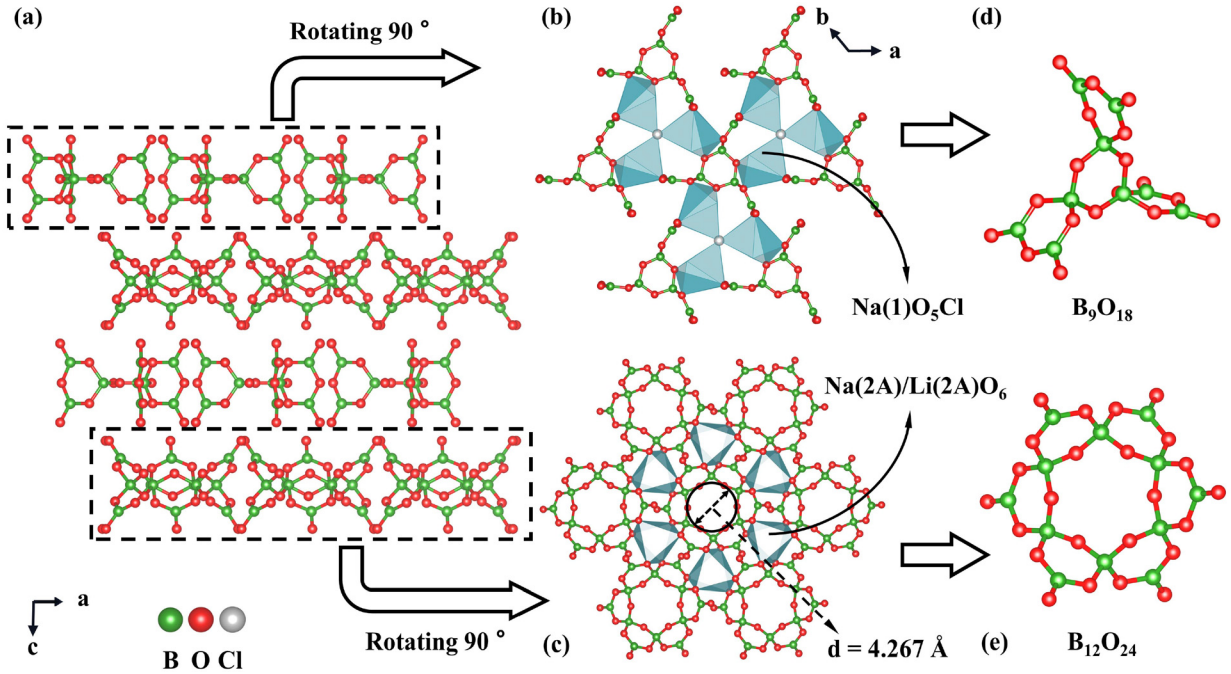

Fig. 3 The crystal structure of LNSBOC. (a) View of the layer-like structure along the *b*-axis; (b) the plane consists of fan-like B_9O_{18} groups; (c) the plane consists of petal-like $B_{12}O_{24}$ groups; (d) isolated B_9O_{18} cluster; (e) isolated $B_{12}O_{24}$ cluster.

joined one after the other. Each tetrahedral BO_4 connects with two neighbouring BO_4 units by the corner-sharing method and shares the other two terminated O atoms with a triangular BO_3. Meanwhile, the six triangular BO_3 units are arranged alternately up and down to form a petal-like structure. By measurement, the diameter of the inner rings of $B_{12}O_{24}$ is approximately 4.267 Å. Furthermore, B_9O_{18} and $B_{12}O_{24}$ groups are separately arranged repeatedly within the *ab* plane, resulting in a two-dimensional (2D) layer-like structure. Within the two pseudo layers, $Na(2A)/Li(2A)O_6$ and $Na(1)O_5Cl$ polyhedra serve as a connection to link the B_9O_{18} and $B_{12}O_{24}$ groups, respectively (Fig. 3) by sharing O atoms. Then the two pseudo layers are arranged alternately along the *c* axis and are bridged by Li(1), Na(1), Sr(1) and Sr(2) atoms as shown in Fig. S1 in the ESI.†

In order to further confirm the accuracy of the crystal structure, the bond valence sum (BVS) calculations for each atom in LNSBOC were performed and the calculation results are listed in Table S1 in the ESI.† The BVS results conformed to the expected oxidation states. Furthermore, EDS was performed on a clean and block single crystal of LNSBOC, which confirmed the presence of the corresponding elements (except Li) in the compound (Fig. S3 in the ESI†). The above measurement results indicate that the crystal structure of LNSBOC is correct.

Structural uniqueness of LNSBOC

After our investigation, the structural uniqueness of LNSBOC is mainly reflected in the following three aspects: the unprecedented coexistence of two highly polymerized (with a number of B atoms of more than six) isolated B–O clusters; the discovery of novel isolated B_9O_{18} clusters acting as FBBs, which further trigger the structural transformation of the space group; and the conflict between the structure of LNSBOC and Pauling's rules. In the following section, these three aspects will be illustrated in detail.

First, LNSBOC possesses the largest two highly polymerized isolated B–O clusters. Based on the inquiry among already reported anhydrous borates, there are only 35 examples of anhydrous borates containing two sorts (or more) of B–O clusters in one structure, which are listed in Table S3 in the ESI.† By comparing the number of listed borates among all the anhydrous borates, the rareness of I-borates with two sorts (or more) of B–O clusters in their structures is shown clearly. Moreover, less than one third of the listed borates (10/35; No. 23–29 and No. 33–35 in Table S3 in the ESI†) contain two sorts of polymerized isolated clusters with a degree of polymerization ≥2, and the title compound is the only example achieving the coexistence of two highly polymerized isolated B–O clusters (polymerization > 6). N_B in Table S3 in the ESI† displays the total number of B atoms in two isolated B–O clusters, which clearly indicates that LNSBOC has the largest two highly polymerized isolated B–O clusters of the reported compounds until now (Fig. 4).

Second, the anhydrous borates with petal-like $B_{12}O_{24}$ clusters have been reported several times in previous studies and are shown as compounds 1–10 in Table S4 in the ESI.† It could be observed that all non-radioactive elements of the alkali and alkaline-earth metals (include Li/Na/K/Rb/Cs and Be/Ca/Sr/Ba) are contained in LNSBOC and these 10 compounds. And almost all of them contain Li^+ and Na^+ cations, only except for

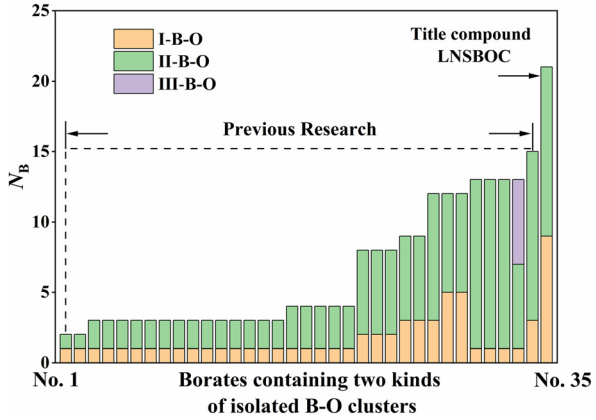

Fig. 4 Chart displaying the statistical N_B (the total number of B atoms in two isolated B–O clusters) data of compounds containing two kinds of isolated B–O clusters. The B–O clusters in a compound are ordered from small to large of boron atoms and named I-B–O, II-B–O, and III-B–O in this order.

$Li_3KB_4O_8/Li_9K_3(B_{12}O_{24})$,[66] which merely contains Li^+. Further structural comparison reveals an obvious rule that all these 10 previous compounds with isolated $B_{12}O_{24}$ clusters crystallize in the same space group, $R\bar{3}$. This rule shows that the entire symmetry of these compounds is seriously influenced by the local symmetry $\bar{3}$ of the $B_{12}O_{24}$ clusters and the type of cation has little effect on that.[66–68] Considering the wide range of variations in the ionic radii of alkali and alkaline-earth metals, which is favourable for adjusting the structure, the related compound system is very valuable to study the effects of the substitution of the same group elements on the properties and structure. In LNSBOC and these 10 compounds, all kinds of B–O clusters (whether $B_{12}O_{24}$ or BO_3 or B_9O_{18}) are respectively arranged as a 2D layer-like structure (Fig. S4 in the ESI†), and they are divided into three classes for further explanation. First, seven compounds (No. 1–7) contain merely lamellar arranged $B_{12}O_{24}$ clusters in their structures, and $LiNa_2Sr_8(B_{12}O_{24})F_6Cl$[66] is shown as an example in Fig. S4a and S4b in the ESI.† Interestingly, although the seven compounds contain different cations with a wide range of ionic radii, their lattice constants remain highly consistent (only except for the *c* axis of $LiNa_2Sr_8(B_{12}O_{24})F_6Cl$), which proves the decisive role of $B_{12}O_{24}$ clusters in the structure. Second, three compounds (No. 8–10) contain isolated $B_{12}O_{24}$ and BO_3 clusters in one crystal structure at the same time, and $Ca_6Li_2Na_8Be_8(BO_3)_8(B_{12}O_{24})F_2$[67] is shown as an example in Fig. S4c and S4d in the ESI.† Although isolated BO_3 is added to the structure, the three compounds maintain the $R\bar{3}$ space group without any change, which further demonstrates the dominance of $B_{12}O_{24}$ clusters in these structures (Fig. S5 in the ESI†). Nevertheless, for the third class, the emergence of the unprecedented isolated B_9O_{18} clusters in the title compound LNSBOC breaks up the monopoly of $B_{12}O_{24}$ in determining the crystal structure, resulting in LNSBOC crystallizing in the space group $P6_3/m$ rather than $R\bar{3}$ like the other 10 compounds. In order to vividly display the structural transformation in the three classes of compounds, the structural variation from $LiNa_2Sr_8(B_{12}O_{24})F_6Cl$ to $Ca_3Li_2Na_8Be_8(BO_3)_8(B_{12}O_{24})F_2$ to LNSBOC is selected as the representation of each class, respectively, and is shown in Fig. S4 in the ESI.† In this section, the effect of the unprecedented isolated B_9O_{18} cluster on the structure of LNSBOC is fully demonstrated through the structural comparison.

Third, the conflict between the structure of LNSBOC and Pauling's rules makes the title compound even more remarkable and rare. First, the existence of face-sharing $Na(1)O_5Cl$ polyhedra (Fig. 2) conflicts with Pauling's third rule that the presence of shared edges, especially of shared faces, in a coordinated structure decreases its stability.[58] According to the assessment of Pauling's rules conducted by George *et al.* in 2020, within about 5000 samples of oxides in the Inorganic Crystal Structure Database, face-sharing polyhedra comprise 1.6% of the polyhedra with a coordination number equal to 8 or smaller. For the coordination polyhedra of Na ions, about 91% of polyhedra are in the connection mode of corner-sharing or edge-sharing.[69] While the face-sharing $Na(1)O_5Cl$ polyhedra conflict with Pauling's third rule, the coexistence of two different kinds of B–O clusters further breaks the limit of Pauling's fifth rule and contributes to the uniqueness of LNSBOC as well. Wang *et al.*[38] analyzed the B–O clusters in $Na_2Be_4(BO_3)_2(B_2O_5)$, γ-$K_3Be_6(BO_3)_3(B_3O_6)_2$, $KBa_2Zn_3(B_3O_6)(B_6O_{13})$ and $Q_{18}Mg_6(B_5O_{10})_3(B_7O_{14})_2F$ (Q = Rb and Cs) and found that the structures of two kinds of isolated clusters in the above compounds are topologically similar, indicating that the coexisting clusters tend to have similar structures to resolve the conflict with Pauling's fifth rule. It is clear that Pauling's fifth rule imposes a restriction on the formation of I-borates containing two types (or more) of isolated B–O clusters. To sum up, the title compound breaks the restriction of Pauling's rules in two aspects, the existence of face-sharing polyhedra and the coexistence of two different B–O clusters, which also shows the uniqueness of its structure.

Design strategies for borates with two polymerized isolated B–O clusters

In order to answer the question of why there are so few borates containing two polymerized isolated B–O clusters and figure out the law of their formation, some empirical analyses from the viewpoint of elements and structures based on previous research and our inquiry were performed.

To start with, the demand for specifically coordinated cations may be the first factor. According to the statistics displayed in Table S3 in the ESI,† a rule could be discovered that most of the I-borates with two sorts (or more) of isolated clusters (33/35) contain four/six-coordinated cationic polyhedra ($[TO_{4/6}]$, T = Be, Zn, Sr, Na, Y, *etc.*) with relatively strong covalent bonds. Likewise, the $Li(1)O_4$, $Na(1)O_5Cl$, $Na(2A)/Li(2A)O_6$ and $Sr(2)O_6$ polyhedra observed in LNSBOC possibly act as a "bond terminator" which not only decomposes the B–O anionic framework to reduce the dimensionality, but also separates the isolated B–O clusters. As shown in Fig. 5a and d,

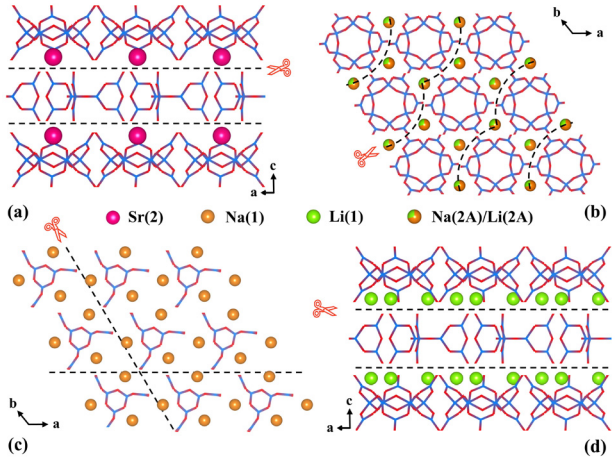

Fig. 5 The distribution of cations in the title compound shows the "bond terminator" role of (a) Sr(2) atoms, (b) Na(2A)/Li(2A) atoms, (c) Na(1) atoms, and (d) Li(1) atoms.

Sr(2) and Li(1) residing in the interstices between the B_9O_{18} and $B_{12}O_{24}$ layers cut off the bridging B–O bonds to separate the two layers. And as for Na(1) and Na(2A)/Li(2A) (Fig. 5b and c), they are respectively located in the interior of the B_9O_{18} and $B_{12}O_{24}$ layers and separate the B–O clusters from each other. Under the action of these four "cation scissors", Li(1), Sr(2), Na(1) and Na(2A)/Li(2A), the structure of LNSBOC eventually appears to be a combination of two kinds of zero-dimensional isolated B–O clusters. Except for $Q_{18}Mg_6(B_5O_{10})_3(B_7O_{14})_2F$ (Q = Rb and Cs) in Wang's work,[38] the title compound provides another instance that further proves that the existence of cations possessing a strong bonding potential is highly indispensable for acquiring borates containing two types (or more) of isolated B–O clusters.[50]

Second, the appropriate ratio of cations/boron could be another significant factor. According to P. Becker's conclusions drawn from statistical analysis,[25] cations could effectively restrain the polymerization of B–O units, indicating that the increasing ratio of cations/boron is undoubtedly in favour of obtaining borates with isolated B–O clusters. In contrast, the decreasing ratio of cations/boron is beneficial for generating polymerized B–O clusters.[50] Therefore, the target to obtain borates containing two polymerized isolated B–O clusters faces an internal contradiction that isolated clusters require the ratio of cations/boron to increase, but the need for polymerization demands the ratio of cations/boron to decrease. Consequently, there must be a compromise on the ratio of cations/boron, which is apparently not easy to realize and further makes the appropriate ratio become a non-negligible factor. To verify the above analysis, the cations/boron ratios of all the 35 compounds were calculated and are listed in Table S3 in the ESI.† It is obvious that the cations/boron ratios of all the 10 borates (No. 23–29 and No. 33–35 in Table S3 in the ESI†) containing two sorts (or more) of polymerized isolated clusters are lower than 1, while the ratio is not less than 1 for the other borates with at least one unpolymerized BO_3 and BO_4 (No. 1–22 and No. 30–32 in Table S3 in the ESI†). For instance, the title compound wboron ra/boron ratio of 0.86 contains polymerized B_9O_{18} and $B_{12}O_{24}$, $\alpha/\beta/\gamma$-$Pb_2Ba_4Zn_4(B_2O_5)(B_6O_{13})_2$[70] with a cations/boron ratio of 0.71 contain polymerized B_2O_5 and B_6O_{13}, and $M_3LiNa_4Be_4(BO_3)_8(B_{12}O_{24})F$ (M = Sr, Cd, Ca) with a cations/boron ratio of 1.20 contain unpolymerized BO_3 and polymerized B_6O_{13}. Therefore, it is clear that an appropriate cations/boron ratio is crucial for the formation of borates with two isolated polymerized B–O clusters.

In view of the above discussion, the existence of specific four/six-coordinated cations possessing relatively strong covalent bonds and appropriate cations/boron ratios which are no less than 0.5 but lower than 1 comprises two indispensable factors for obtaining borates with two polymerized isolated B–O clusters. And the conclusion could also be seen as an effective strategy for designing this kind of compound. Nevertheless, the above discussion is merely based on a summary of extant compounds, and the insufficiency of the examples makes the discussion merely empirical. We look forward to the further discovery of I-borates with two polymerized isolated B–O clusters to enrich the structural diversity of borates and verify the discussion to make it theoretical.

UV–Vis–NIR diffuse reflectance spectroscopy

The UV–Vis–NIR diffuse reflectance spectrum shown in Fig. 6 illustrates that the reflectance of LNSBOC is 48% at 200 nm, which shows that the title compound has a UV cutoff edge below 200 nm. The result is comparable with those of related compounds including $LiNa_2Sr_8(B_{12}O_{24})F_6Cl$ (<190 nm), $Li_6Na_2Ba_3(B_{12}O_{24})$[71] (<190 nm) and $Sr_3LiNa_4Be_4(B_{10}O_{24})F$ (<200 nm). The short UV cutoff edge could be partially attributed to the existence of alkali and alkaline-earth metal cations, which get rid of the effect of *d–d* and *f–f* transitions. The UV–Vis–NIR diffuse reflectance spectrum indicates that LNSBOC may possess application potential in the deep-UV region.

IR spectroscopy

The infrared spectrum shown in Fig. S6 in the ESI† was obtained to verify the coordination environment of B–O groups in the title compound, and the assignments for the

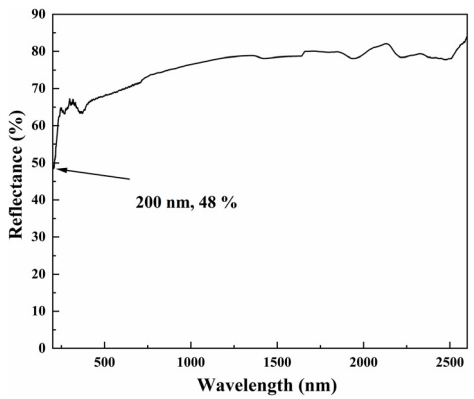

Fig. 6 The UV–vis–NIR optical spectrum of LNSBOC.

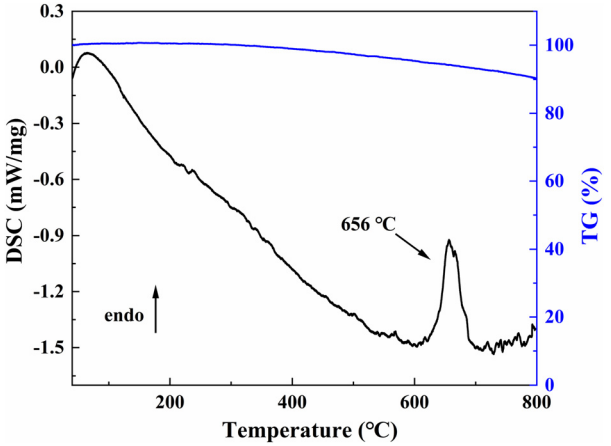

Fig. 7 The TG-DSC curves of LNSBOC.

absorption peaks are listed in Table S5 in the ESI.† The result conforms to the crystal structure of LNSBOC and the spectrum is similar to those of other compounds containing $B_{12}O_{24}$ groups.[67,68,72–79]

TG and DSC analyses

On the TG-DSC curves of LNSBOC shown in Fig. 7, an endothermic peak emerges near 656 °C during the heating process with no obvious weight loss, which indicates that the compound is quite stable. The endothermic peak could be ascribed to the melting process of LNSBOC. To further research its thermodynamic behavior, the polycrystalline sample of LNSBOC was put in a platinum crucible and then placed in a single crystal growth furnace and heated to 800 °C, then slowly cooled to room temperature. Powder XRD analysis was conducted again on the ground crystallized product. The analysis of the XRD reveals that the entire solid product exhibits a diffraction pattern different from that of the initial pure powder, as shown in Fig. S7 in the ESI.† The pattern of the melted samples was analyzed by comparison with relevant XRD patterns, and the results show that SrB_2O_4 (PDF#15-0779) is the major component of the molten products, and a small amount of undecomposed LNSBOC and some other small peaks that could not be recognized also contribute to the pattern. The above analysis further indicates that LNSBOC is an incongruent melting compound.

Conclusions

In conclusion, a new borate, LNSBOC, was successfully obtained *via* a high-temperature solution method in an open system. It crystallizes in the centrosymmetric space group $P6_3/m$ and contains two large isolated B–O clusters, B_9O_{18} and $B_{12}O_{24}$, acting as fundamental building blocks (FBBs). To the best of our knowledge, the title compound is the only borate that exhibits the coexistence of the largest two highly polymerized isolated B–O clusters (B_9O_{18} and $B_{12}O_{24}$) among all the reported borates. Meanwhile, the isolated B_9O_{18} unit is a novel FBB obtained for the first time. LNSBOC displays a wide transparency region with a deep-UV cutoff edge below 200 nm. Furthermore, the factors affecting the formation of borates with two polymerized isolated B–O clusters have been empirically analyzed, and the corresponding design strategies are proposed from the viewpoint of structures and elements as well. The design strategies will be helpful to discover more borates with two polymerized isolated B–O clusters to further enrich the structural chemistry of borates.

Conflicts of interest

The authors declare that they have no conflict of interest.

Acknowledgements

This work was supported by the National Natural Science Foundation of China (51872325, 61835014, and 51972336), the Shanghai Cooperation Organization Science and Technology Partnership Program (2020E01039), the Xinjiang Tianshan Youth Program–Outstanding Young Science and Technology Talents (2020Q004), the CAS Youth Interdisciplinary Team (JCTD-2021-18), the West Light Foundation of CAS (2021-XBQNXZ-004), the Scientific Instrument Developing Project, CAS (YJKYYQ20210033, GJJSTD20200007), the Key Research Program of Frontier Sciences, CAS (ZDBS-LY-SLH035), the International Partnership Program of CAS (1A1365kysb20200008), the Xinjiang Major Science and Technology Project (2021A01001), and the Science and Technology Service Network Initiative of CAS (KFJ-STS-QYZD-130).

References

1 P. Becker, Borate materials in nonlinear optics, *Adv. Mater.*, 1998, **10**, 979–992.
2 P. S. Halasyamani and K. R. Poeppelmeier, Noncentrosymmetric oxides, *Chem. Mater.*, 1998, **10**, 2753–2769.
3 X. L. Chen and K. M. Ok, Metal oxyhalides: An emerging family of nonlinear optical materials, *Chem. Sci.*, 2022, **13**, 3942–3956.
4 C. T. Chen, N. Ye, J. Lin, J. Jiang, W. R. Zeng and B. C. Wu, Computer-assisted search for nonlinear optical crystals, *Adv. Mater.*, 1999, **11**, 1071–1078.
5 F. Kong, H. L. Jiang, T. Hu and J. G. Mao, CsB_3GeO_7 and $K_2B_2Ge_3O_{10}$: Explorations of new second-order nonlinear optical materials in the borogermanate systems, *Inorg. Chem.*, 2008, **47**, 10611–10617.
6 J. H. Huang, C. C. Jin, P. L. Xu, P. F. Gong, Z. S. Lin, J. W. Cheng and G. Y. Yang, $Li_2CsB_7O_{10}(OH)_4$: A deep-ultraviolet nonlinear-optical mixed-alkaline borate constructed

by unusual heptaborate anions, *Inorg. Chem.*, 2019, **58**, 1755–1758.

7 Y. Yang, X. Y. Dong, Z. H. Yang and S. L. Pan, $CsBaB_9O_{15}$: A high performance ultraviolet nonlinear optical material activated by the peculiar double layered configuration, *Sci. Bull.*, 2021, **66**, 2165–2169.

8 P. F. Gong, X. M. Liu, L. Kang and Z. S. Lin, Inorganic planar π-conjugated groups in nonlinear optical crystals: Review and outlook, *Inorg. Chem. Front.*, 2020, **7**, 839–852.

9 G. Q. Shi, Y. Wang, F. F. Zhang, B. B. Zhang, Z. H. Yang, X. L. Hou, S. L. Pan and K. R. Poeppelmeier, Finding the next deep-ultraviolet nonlinear optical material: $NH_4B_4O_6F$, *J. Am. Chem. Soc.*, 2017, **139**, 10645–10648.

10 X. L. Chen, H. Jo and K. M. Ok, Lead mixed oxyhalides satisfying all fundamental requirements for high-performance mid-Infrared nonlinear optical materials, *Angew. Chem., Int. Ed.*, 2020, **59**, 7514–7520.

11 G. H. Zou and K. M. Ok, Novel ultraviolet (UV) nonlinear optical (NLO) materials discovered by chemical substitution-oriented design, *Chem. Sci.*, 2020, **11**, 5404–5409.

12 Y. Yang, S. Z. Huang and S. L. Pan, $K_3Sr_3Li_2Al_4B_6O_{20}F$: A competitive nonlinear optical crystal for generation of 266 nm laser, *J. Mater. Chem. C*, 2022, DOI: **10.1039/D2TC02073D**.

13 Y. Yang and S. L. Pan, Ion-induced structural and optical performance evolution in LBO-like crystals: Experimental and theoretical investigation, *Inorg. Chem. Front.*, 2018, **5**, 2955–2963.

14 C. M. Huang, M. Mutailipu, F. F. Zhang, K. J. Griffith, C. Hu, Z. H. Yang, J. M. Griffin, K. R. Poeppelmeier and S. L. Pan, Expanding the chemistry of borates with functional $[BO_2]^-$ anions, *Nat. Commun.*, 2021, **12**, 2597.

15 S. Z. Huang, Y. Yang, J. B. Chen, W. Q. Jin, S. C. Cheng, Z. H. Yang and S. L. Pan, "Removing center"—An effective structure design strategy for nonlinear optical crystals, *Chem. Mater.*, 2022, **34**, 2429–2438.

16 H. A. Höppe, $Gd_4(BO_2)O_5F$—A gadolinium borate fluoride oxide comprising a linear BO_2 moiety, *Z. Naturforsch., B: J. Chem. Sci.*, 2015, **70**, 769–774.

17 B. B. Zhang, G. Q. Shi, Z. H. Yang, F. F. Zhang and S. L. Pan, Fluorooxoborates: Beryllium-free deep-ultraviolet nonlinear optical materials without layered growth, *Angew. Chem., Int. Ed.*, 2017, **56**, 3916–3919.

18 Y. H. Zhang, F. M. Li, R. Yang, Y. Yang, F. F. Zhang, Z. H. Yang and S. L. Pan, $Rb_5Ba_2(B_{10}O_{17})_2(BO_2)$: The formation of unusual functional $[BO_2]^-$ in borates with deep-ultraviolet transmission window, *Sci. China: Chem.*, 2022, **65**, 719–725.

19 X. F. Wang, Y. Wang, B. B. Zhang, F. F. Zhang, Z. H. Yang and S. L. Pan, CsB_4O_6F: A congruent-melting deep-ultraviolet nonlinear optical material by combining superior functional units, *Angew. Chem., Int. Ed.*, 2017, **56**, 14119–14123.

20 M. Mutailipu, M. Zhang, B. B. Zhang, L. Y. Wang, Z. H. Yang, X. Zhou and S. L. Pan, $SrB_5O_7F_3$ functionalized with $[B_5O_9F_3]^{6-}$ chromophores: Accelerating the rational design of deep-ultraviolet nonlinear optical materials, *Angew. Chem., Int. Ed.*, 2018, **57**, 6095–6099.

21 X. F. Wang, F. F. Zhang, L. Gao, Z. H. Yang and S. L. Pan, Nontoxic KBBF family member $Zn_2BO_3(OH)$: Balance between beneficial layered structure and layer tendency, *Adv. Sci.*, 2019, **6**, 1901679.

22 P. Burns, J. Grice and F. Hawthorne, Borate minerals. 1. polyheral clusters and fundamental building-blocks, *Can. Mineral.*, 1995, **33**, 1131–1151.

23 H. Strunz, Classification of borate minerals, *Eur. J. Mineral.*, 1997, **9**, 225–232.

24 M. Touboul, N. Penin and G. Nowogrocki, Borates: A survey of main trends concerning crystal-chemistry, polymorphism and dehydration process of alkaline and pseudo-alkaline borates, *Solid State Sci.*, 2003, **5**, 1327–1342.

25 P. Becker, A contribution to borate crystal chemistry: Rules for the occurrence of polyborate anion types, *Z. Kristallogr. – Cryst. Mater.*, 2001, **216**, 523–533.

26 Y. Wang, B. B. Zhang, Z. H. Yang and S. L. Pan, Cation-tuned synthesis of fluorooxoborates: Towards optimal deep-ultraviolet nonlinear optical materials, *Angew. Chem., Int. Ed.*, 2018, **57**, 2150–2154.

27 Z. Z. Zhang, Y. Wang, B. B. Zhang, Z. H. Yang and S. L. Pan, Polar fluorooxoborate, NaB_4O_6F: A promising material for ionic conduction and nonlinear optics, *Angew. Chem., Int. Ed.*, 2018, **57**, 6577–6581.

28 S. S. Li, X. M. Liu, H. P. Wu, Z. F. Song, H. W. Yu, Z. S. Lin, Z. G. Hu, J. Y. Wang and Y. C. Wu, $Ba_4Ca(B_2O_5)_2F_2$: π-conjugation of B_2O_5 in the planar pentagonal layer achieving large second harmonic generation of pyro-borate, *Chem. Sci.*, 2021, **12**, 13897–13901.

29 X. Y. Dong, Q. Jing, Y. J. Shi, Z. H. Yang, S. L. Pan, K. R. Poeppelmeier, J. Young and J. M. Rondinelli, $Pb_2Ba_3(BO_3)_3Cl$: A material with large SHG enhancement activated by Pb-chelated BO_3 groups, *J. Am. Chem. Soc.*, 2015, **137**, 9417–9422.

30 K. M. Ok, Toward the rational design of novel noncentrosymmetric materials: Factors influencing the framework structures, *Acc. Chem. Res.*, 2016, **49**, 2774–2785.

31 Z. G. Xia and K. R. Poeppelmeier, Chemistry-inspired adaptable framework structures, *Acc. Chem. Res.*, 2017, **50**, 1222–1230.

32 H. W. Yu, W. G. Zhang, J. Young, J. M. Rondinelli and P. S. Halasyamani, Design and synthesis of the beryllium-free deep-ultraviolet nonlinear optical material $Ba_3(ZnB_5O_{10})PO_4$, *Adv. Mater.*, 2015, **27**, 7380–7385.

33 H. L. Pei, Q. Wei, L. Sun and G. Y. Yang, $[M(1,2\text{-dap})_3][B_{10}O_{13}(OH)_6]$ (M = Co, Ni): Two new borates containing $[B_{10}O_{13}(OH)_6]^{2-}$ cluster units, *J. Cluster Sci.*, 2018, **29**, 49–55.

34 G. Y. Yang and K. C. Wu, Two-dimensional deep-ultraviolet beryllium-free $KBe_2BO_3F_2$ family nonlinear-optical monolayer, *Inorg. Chem.*, 2018, **57**, 7503–7506.

35 G. H. Zou, C. S. Lin, H. Jo, G. Nam, T.-S. You and K. M. Ok, Pb_2BO_3Cl: A tailor-made polar lead borate chloride with very strong second harmonic generation, *Angew. Chem., Int. Ed.*, 2016, **55**, 12078–12082.

36 Z. J. Wang, H. M. Qiao, R. B. Su, B. Hu, X. M. Yang, C. He and X. F. Long, $Mg_3B_7O_{13}Cl$: A new quasi-phase matching crystal in the deep-ultraviolet region, *Adv. Funct. Mater.*, 2018, **28**, 1804089.

37 L. Qi, Z. H. Chen, X. R. Shi, X. D. Zhang, Q. Jing, N. Li, Z. Q. Jiang, B. B. Zhang and M.-H. Lee, $A_3BBi(P_2O_7)_2$ (A = Rb, Cs; B = Pb, Ba): Isovalent cation substitution to sustain large second-harmonic generation responses, *Chem. Mater.*, 2020, **32**, 8713–8723.

38 Z. Wang, M. Zhang, X. Su, S. L. Pan, Z. H. Yang, H. Zhang and L. Liu, $Q_{18}Mg_6(B_5O_{10})_3(B_7O_{14})_2F$ (Q = Rb and Cs): New borates containing two large isolated polyborate anions with similar topological structures, *Chem. – Eur. J.*, 2015, **21**, 1414–1419.

39 J. J. Zhou, Y. Q. Liu, H. P. Wu, H. W. Yu, Z. S. Lin, Z. G. Hu, J. Y. Wang and Y. C. Wu, $CsZn_2BO_3X_2$ (X_2 = F_2, Cl_2, and FCl): A series of beryllium-free deep-ultraviolet nonlinear-optical crystals with excellent properties, *Angew. Chem., Int. Ed.*, 2020, **59**, 19006–19010.

40 C. T. Chen and G. Z. Liu, Recent advances in nonlinear optical and electro-optical materials, *Annu. Rev. Mater. Sci.*, 1986, **16**, 203–243.

41 C. T. Chen, G. L. Wang, X. Y. Wang and Z. Y. Xu, Deep-UV nonlinear optical crystal $KBe_2BO_3F_2$—Discovery, growth, optical properties and applications, *Appl. Phys. B*, 2009, **97**, 9–25.

42 R. K. Li and Y. Y. Ma, Chemical engineering of a birefringent crystal transparent in the deep UV range, *CrystEngComm*, 2012, **14**, 5421–5424.

43 B. C. Wu, D. Y. Tang, N. Ye and C. T. Chen, Linear and nonlinear optical properties of the $KBe_2BO_3F_2$ (KBBF) crystal, *Opt. Mater.*, 1996, **5**, 105–109.

44 R. Q. Liu, H. P. Wu, H. W. Yu, Z. G. Hu, J. Y. Wang and Y. C. Wu, $K_5Mg_2La_3(BO_3)_6$: An efficient, deep-ultraviolet nonlinear optical material, *Chem. Mater.*, 2021, **33**, 4240–4246.

45 A. D. Mighell, A. Perloff and S. Block, The crystal structure of the high temperature form of barium borate, $BaO.B_2O_3$, *Acta Crystallogr.*, 1966, **20**, 819–823.

46 S. F. Wu, G. F. Wang, J. L. Xie, X. Q. Wu, Y. F. Zhang and X. Lin, Growth of large birefringent α-BBO crystal, *J. Cryst. Growth*, 2002, **245**, 84–86.

47 X. F. Lu, Z. H. Chen, X. R. Shi, Q. Jing and M.-H. Lee, Two pyrophosphates with large birefringences and second-harmonic responses as ultraviolet nonlinear optical materials, *Angew. Chem., Int. Ed.*, 2020, **59**, 17648–17656.

48 Z. Wang, M. Zhang, S. L. Pan, Z. H. Yang, H. Zhang, B. B. Zhang, Y. Wang, J. Kang and X. X. Lin, Exploring the influence of cationic skeletons on the arrangement of isolated BO_3 groups based on $RbMgBO_3$, $CsZn_4(BO_3)_3$ and $Cs_4Mg_4(BO_3)_4$, *New J. Chem.*, 2014, **38**, 3035–3041.

49 R. K. Li and P. Chen, Cation coordination control of anionic group alignment to maximize SHG effects in the $BaMBO_3F$ (M = Zn, Mg) series, *Inorg. Chem.*, 2010, **49**, 1561–1565.

50 M. Mutailipu, K. R. Poeppelmeier and S. L. Pan, Borates: A rich source for optical materials, *Chem. Rev.*, 2021, **121**, 1130–1202.

51 G. H. Yuan and D. F. Xue, Crystal chemistry of borates: The classification and algebraic description by topological type of fundamental building blocks, *Acta Crystallogr., Sect. B: Struct. Sci.*, 2007, **63**, 353–362.

52 C. T. Chen, Y. B. Wang, B. C. Wu, K. C. Wu, W. L. Zeng and L. H. Yu, Design and synthesis of an ultraviolet-transparent nonlinear optical crystal $Sr_2Be_2B_2O_7$, *Nature*, 1995, **373**, 322–324.

53 S. G. Zhao, P. F. Gong, L. Bai, X. Xu, S. Q. Zhang, Z. H. Sun, Z. S. Lin, M. C. Hong, C. T. Chen and J. H. Luo, Beryllium-free $Li_4Sr(BO_3)_2$ for deep-ultraviolet nonlinear optical applications, *Nat. Commun.*, 2014, **5**, 4019.

54 C. T. Chen, B. C. Wu, A. D. Jiang and G. M. You, A new-type ultraviolet SHG crystal—β-BaB_2O_4, *Sci. China, Ser. B: Chem., Life Sci., Earth Sci.*, 1985, **20**, 235–243.

55 S. F. Jin, G. M. Cai, W. Y. Wang, M. He, S. C. Wang and X. L. Chen, Stable oxoborate with edge-sharing BO_4 tetrahedra synthesized under ambient pressure, *Angew. Chem., Int. Ed.*, 2010, **49**, 4967–4970.

56 Y. Yang, S. L. Pan, J. Han, X. L. Hou, Z. X. Zhou, W. W. Zhao, Z. H. Chen and M. Zhang, A new lithium rubidium borate $Li_6Rb_5B_{11}O_{22}$ with isolated $B_{11}O_{22}$ building blocks, *Cryst. Growth Des.*, 2011, **11**, 3912–3916.

57 X. A. Chen, J. Y. Yue, X. A. Chang and W. Q. Xiao, Synthesis and characterization of a new borate $Ba_6Al_4B_{14}O_{33}$ with building blocks of AlO_4, Al_4O_{14}, BO_3, B_6O_{14}, and B_6O_{13}, *J. Solid State Chem.*, 2017, **245**, 174–183.

58 J. K. Burdett and T. J. McLarnan, An orbital interpretation of Pauling's rules, *Am. Mineral.*, 1984, **69**, 601–621.

59 X. A. Chen, Y. J. Chen, C. Sun, X. A. Chang and W. Q. Xiao, Synthesis, crystal structure, spectrum properties, and electronic structure of a new three-borate $Ba_4Na_2Zn_4(B_3O_6)_2(B_{12}O_{24})$ with two isolated types of blocks: 3[3Δ] and 3[2Δ + 1T], *J. Alloys Compd.*, 2013, **568**, 60–67.

60 *SAINT, Version 7.60A*, Bruker Analytical X-ray Instruments, Inc., Madison, WI, 2008.

61 O. Dolomanov, L. Bourhis, R. Gildea, J. Howard and H. Puschmann, OLEX2: A complete structure solution, refinement and analysis program, *J. Appl. Crystallogr.*, 2009, **42**, 339–341.

62 G. Sheldrick, A short history of SHELX, *Acta Crystallogr., Sect. A: Found. Crystallogr.*, 2008, **64**, 112–122.

63 A. Spek, Single-crystal structure validation with the program PLATON, *J. Appl. Crystallogr.*, 2003, **36**, 7–13.

64 C. L. Christ and J. R. Clark, A crystal-chemical classification of borate structures with emphasis on hydrated borates, *Phys. Chem. Miner.*, 1977, **2**, 59–87.

65 X. Y. Dong, H. P. Wu, Y. J. Shi, H. W. Yu, Z. H. Yang, B. B. Zhang, Z. H. Chen, Y. Yang, Z. J. Huang, S. L. Pan and Z. X. Zhou, $Na_{11}B_{21}O_{36}X_2$ (X = Cl, Br): Halogen sodium borates with a new graphene-like borate double layer, *Chem. – Eur. J.*, 2013, **19**, 7338–7341.

66 H. P. Wu, H. W. Yu, S. L. Pan, A. Q. Jiao, J. Han, K. Wu, S. J. Han and H. Y. Li, New type of complex alkali and alkaline earth metal borates with isolated $(B_{12}O_{24})^{12-}$ anionic group, *Dalton Trans.*, 2014, **43**, 4886–4891.

67 S. Y. Luo, W. J. Yao, P. F. Gong, J. Y. Yao, Z. S. Lin and C. T. Chen, $Ca_3Na_4LiBe_4B_{10}O_{24}F$: A new beryllium borate with a unique beryl borate $\infty^2[Be_8B_{16}O_{40}F_2]$ layer intrabridged by $[B_{12}O_{24}]$ groups, *Inorg. Chem.*, 2014, **53**, 8197–8199.

68 X. S. Wang, L. J. Liu, M. J. Xia, X. Y. Wang and C. T. Chen, Two isostructural multi-metal borates: Syntheses, crystal structures and characterizations of $M_3LiNa_4Be_4B_{10}O_{24}F$ (M = Sr, Cd), *Chin. J. Struct. Chem.*, 2015, **34**, 1617–1625.

69 J. George, D. Waroquiers, D. Di Stefano, G. Petretto, G.-M. Rignanese and G. Hautier, The limited predictive power of the Pauling rules, *Angew. Chem., Int. Ed.*, 2020, **59**, 7569–7575.

70 H. W. Yu, H. P. Wu, Q. Jing, Z. H. Yang, P. S. Halasyamani and S. L. Pan, Polar polymorphism: α-, β-, and γ-$Pb_2Ba_4Zn_4B_{14}O_{31}$ – Synthesis, characterization, and nonlinear optical properties, *Chem. Mater.*, 2015, **27**, 4779–4788.

71 S. J. Chen, S. L. Pan, W. W. Zhao, Z. H. Yang, H. P. Wu and Y. Yang, Synthesis, crystal structure and characterization of a new compound, $Li_3NaBaB_6O_{12}$, *Solid State Sci.*, 2012, **14**, 1186–1190.

72 H. P. Wu, H. W. Yu, Z. H. Yang, X. L. Hou, X. Su, S. L. Pan, K. R. Poeppelmeier and J. M. Rondinelli, Designing a deep-ultraviolet nonlinear optical material with a large second harmonic generation response, *J. Am. Chem. Soc.*, 2013, **135**, 4215–4218.

73 T. Baiheti, S. J. Han, B. Bashir, Z. H. Yang, Y. Wang, H. H. Yu and S. L. Pan, Four new deep ultraviolet borates with isolated $B_{12}O_{24}$ groups: Synthesis, structure, and optical properties, *J. Solid State Chem.*, 2019, **273**, 112–116.

74 M. Abudoureheman, S. J. Han, Y. Wang, Q. Liu, Z. H. Yang and S. L. Pan, Three mixed-alkaline borates: $Na_2M_2B_{20}O_{32}$ (M = Rb, Cs) with two Interpenetrating three-dimensional B-O networks and $Li_4Cs_4B_{40}O_{64}$ with fundamental building block $B_{40}O_{77}$, *Inorg. Chem.*, 2017, **56**, 13456–13463.

75 S. J. Han, Y. Wang, S. L. Pan, X. Y. Dong, H. P. Wu, J. Han, Y. Yang, H. W. Yu and C. Y. Bai, Noncentrosymmetric versus centrosymmetric: Influence of the Na^+ substitution on structural transition and second-harmonic generation property, *Cryst. Growth Des.*, 2014, **14**, 1794–1801.

76 G. Blasse and G. P. M. Van Den Heuvel, Some optical properties of tantalum borate (tabo4), a compound with unusual coordinations, *Phys. Status Solidi A*, 1973, **19**, 111–117.

77 Z. H. Liu, S. Y. Gao and S. P. Xia, FT-IR spectroscopic study of phase transformation of chloropinnoite in boric acid solution at 303 K, *Spectrochim. Acta, Part A*, 2003, **59**, 265–270.

78 X. A. Chen, C. Y. Yang, Z. P. Chu, X. A. Chang, H. G. Zang and W. Q. Xiao, Synthesis, spectrum properties, and crystal structure of a new pentaborate, $Na_{2.18}K_{0.82}SrB_5O_{10}$, *J. Chem. Crystallogr.*, 2011, **41**, 816–822.

79 H. W. Huang, L. J. Liu, S. F. Jin, W. J. Yao, Y. H. Zhang and C. T. Chen, Deep-ultraviolet nonlinear optical materials: $Na_2Be_4B_4O_{11}$ and $LiNa_5Be_{12}B_{12}O_{33}$, *J. Am. Chem. Soc.*, 2013, **135**, 18319–18322.